Multiseeded Fuzzy Segmentation on the Face Centered Cubic Grid

Carvalho, B. M.[1]*, Garduño, E.[1], and Herman, G. T.[2]

[1] University of Pennsylvania,Philadelphia PA 19104, USA
[2] Temple University, Philadelphia PA 19122, USA

Summary. Fuzzy connectedness has been effectively used to segment out objects in volumes containing noise and/or shading. Multiseeded fuzzy segmentation is a generalized approach that produces a unique simultaneous segmentation of multiple objects. Fcc (face centered cubic) grids are grids formed by rhombic dodecahedral voxels that can be used to represent volumes with fewer elements than a normal cubic grid. Tomographic reconstructions (PET and CT) are used to evaluate the accuracy and speed of the algorithm.

keywords: multisegmentation, fuzzy conectedness, fuzzy graph, FCC grid, PET, CT.

1 Introduction

Segmentation is the process of recognizing objects in an image. If the image in question is corrupted by noise or the objects to be recognized are defined not only by the intensity assigned to the pixels belonging to them (i.e., they are defined by some textural property), then thresholding is not an appropriate method of segmentation but the concept of fuzzy connectedness can be successfully used to segment images [1–4]. The concept of fuzzy connectedness was introduced by Rosenfeld [5]. Our approach (introduced in [6]) is based on [7], but is generalized to arbitrary digital spaces [8].

In the fuzzy connectedness context we define a *chain* as a sequence of voxels (short for volume elements) and its *links* as the pairs of consecutive voxels. The *strength* of any link is automatically determined according to statistical properties of the links selected by the user as connecting two voxels within the object of interest. The strength of a chain is equal to the strength of its weakest link. The *fuzzy connectedness* between any pair of voxels is the

* This research is supported by NIH Grant HL28438 (BMC, EG and GTH), NFS Grant DMS96122077 (GTH), CAPES-BRASÍLIA-BRAZIL (BMC) and CONACyT-Mexico (EG).

S. Singh, N. Murshed, and W. Kropatsch (Eds.): ICAPR 2001, LNCS 2013, pp. 339–348, 2001.

strength of the strongest chain between them. In multiseeded segmentation we generalize this approach by allowing each object to have its own definition of strength for the links and its own set of seed voxels. Then, each object is defined as the set of voxels that are connected in a stronger way to one of the seeds of that object than to any of the seeds of the other objects.

As this high-level description of the method suggests, the most computationally expensive task in determining these objects based on the pre-selected seeds is the calculation of the multiple fuzzy connectedness of all the voxels to the seed voxels. This involves finding the strongest chain between a voxel and one or more seed voxels. We make use of the greedy algorithm presented in [6] to efficiently achieve the segmentation of PET (Positron Emission Tomography) and CT (Computed Tomography) volumes on the fcc grid.

In Section 2 we describe in detail the theory and the algorithm which performs the multiseeded fuzzy segmentation. Section 3 describes the fcc grid and its advantages in volume representation when compared to the simple cubic grid. In Section 4 we describe the experiments used to evaluate the multiseeded fuzzy segmentation algorithm. Finally, in Section 5 we present our conclusions.

2 Multiseeded Fuzzy Segmentation

For a positive integer M, an *M-semisegmentation* of a set V (of *spels*, short for spatial element) is a function σ which maps each $c \in V$ into an $(M+1)$-dimensional vector $\sigma^c = (\sigma_0^c, \sigma_1^c, \cdots, \sigma_M^c)$, such that $\sigma_0^c \in [0,1]$ (i.e., it is nonnegative but not greater than 1) and for at least one m, in the range $1 \le m \le M$, $\sigma_m^c = \sigma_0^c$ and for all other m it is either 0 or σ_0^c. We say that σ is an M-segmentation if, for every spel c, σ_0^c is positive.

A *fuzzy spel affinity* on V is a function $\psi : V^2 \to [0,1]$. We think of (c,d) as a *link* and of $\psi(c,d)$ as its *ψ-strength*. (In some of the previous literature it was also assumed that $\psi(c,d) = \psi(d,c)$; we do not need this restriction.) We define a chain in $U(\subseteq V)$ from $c^{(0)}$ to $c^{(K)}$ to be a sequence $\langle c^{(0)}, \cdots, c^{(K)} \rangle$ of spels in U and the ψ-strength of this chain as the ψ-strength of its weakest link $\left(c^{(k-1)}, c^{(k)}\right)$, $1 \le k \le K$. (In case $K = 0$, the ψ-strength is defined to be 1.) We say that U is *ψ-connected* if for every pair of distinct spels in U there is a chain in U of positive ψ-strength from the first spel of the pair to the second.

If there are multiple objects to be segmented, it is reasonable that each should have its own fuzzy spel affinity [9], which leads to the following. An *M-fuzzy graph* is a pair $(V, \boldsymbol{\Psi})$, where V is a nonempty finite set and $\boldsymbol{\Psi} = (\psi_1, \cdots, \psi_M)$ and ψ_m (for $1 \le m \le M$) is a fuzzy spel affinity such that

V is $(min_{1\leq m\leq M}\psi_m)$-connected. (This is defined by $(min_{1\leq m\leq M}\psi_m)(c,d) = min_{1\leq m\leq M}\psi_m(c,d)$.) For an M-semisegmentation σ of V and for $1 \leq m \leq M$, the chain $\langle c^{(0)}, \cdots, c^{(K)} \rangle$ is said to be a σm-chain if $\sigma_m^{c^{(k)}} > 0$, for $0 \leq k \leq K$. Further, for $U \subseteq V$, $W \subseteq V$ and $c \in V$, we use $\mu_{\sigma,m,U,W}(c)$ to denote the maximal ψ-strength of a σm-chain in U from a spel in W to c. (This is equal to 0 if there is no such chain.)

Theorem. If (V, Ψ) is an M-fuzzy graph and, for $1 \leq m \leq M$, V_m is a subset (of *seed spels*) of V such that at least one of these subsets is nonempty, then there exists a unique M-semisegmentation (which is, in fact, an M-segmentation) σ of V with the following property. For every $c \in V$, if for $1 \leq n \leq M$

$$s_n^c = \begin{cases} 1, & \text{if } c \in V_n, \\ max_{d\in V}(min(\mu_{\sigma,n,V,V_n}(d), \psi_n(d,c))), & \text{otherwise,} \end{cases} \tag{1}$$

then for $1 \leq m \leq M$

$$\sigma_m^c = \begin{cases} s_m^c, \text{ if } s_m^c \geq s_n^c \text{ for } 1 \leq n \leq M, \\ 0, \quad \text{otherwise.} \end{cases} \tag{2}$$

The fact that if σ is a M-semisegmentation that has this property, then σ is in fact unique and a M-segmentation is proved in [6]. In the same paper a greedy algorithm is provided which receives as input M sets of spels (V_m, for $1 \leq m \leq M$) and updates, during its execution, the current M-semisegmentation σ; producing, at the end, an M-semisegmentation that satisfies the property of the Theorem.

An intuitive picture of our algorithm is the following. There are M competing armies (one corresponding to each object). Initially they each have full strength and they occupy their respective seed spels. All armies try to increase their respective territories, but the moving from a spel to another one reduces the strength of the soldiers to be the minimum of their strength on the previous spel and the affinity (for that army or object) between the spels. At any given time, a spel will be occupied by the soldiers of the armies which were not weaker than any other soldiers who reached that spel by that time. Eventually a steady state is reached; this steady state satisfies the property of the Theorem. The sequential algorithm simulates this intuitively described parallel behaviour of the M armies.

A priority queue H of spels c is used by the algorithm. This queue, with associated keys σ_0^c, is a *max-queue*, meaning that the "first" element of the queue is the element with the maximal key (we denote this value by Maximum-Key(H), that returns 0 if H is empty). The algorithm keeps inserting spels into the queue (each spel is inserted exactly once using the

operation $H \leftarrow H \cup \{c\}$) and will eventually be extracted from the queue (using the operation Remove-Max(H) that removes the element at the top of the queue), at which time, this spel c already has the final value for the vector σ^c. The real variable l holds the current value of Maximum-Key(H) and the spels are removed from H in a non-increasing order of their keys σ_0^c.

In the initialization phase (steps 1-9 of algorithm), all spels have the values σ_m^c set to 0 for $0 \leq m \leq M$. Then, for every spel c belonging to one of the seed spel sets V_m, c is inserted into H and both σ_0^c and σ_m^c are set to 1. After this step, l is also set to 1.

After the initialization, the following conditions are satisfied:

1. σ is an M-semisegmentation of V.
2. A spel c is in H if, and only if, $\sigma_0^c > 0$.
3. $l =$ Maximum-Key(H).
4. For $1 \leq m \leq M$, $V_m = \{c \in H \mid \sigma_m^c = l\}$.

At the beginning of the main loop (steps 10-28), conditions 1 to 4 are satisfied, and this loop is executed for decreasing values of l until this variable is set to 0, at which point the priority queue is empty and the algorithm terminates.

The first part of the main loop (steps 10-23) is responsible for updating the values of σ_m^c. A value is updated when a σm-chain with a ψ_m-strength greater than the old value from an element of the seed spels in the initial V_m to c is found, and the value σ_m^c is set to 0 if it is found, for an $n \neq m$, that there is a σn-chain from an element of the seed spels in the initial V_n to c with a ψ_n-strength greater than the old value of σ_m^c. The second part of the loop (steps 24-28) is responsible for removing the spels c with maximum keys ($\sigma_0^c = l$), assigning to l the value of the new maximum key and setting V_m to be the set of spels c with $\sigma_m^c = l$, for $1 \leq m \leq M$, thus satisfying the conditions 3 and 4. The algorithm, using the conventions adopted in [10], is described on the next page.

3 The Fcc Grid

Now we explain why we use the fcc grid, by comparing it to the cubic grid and showing the advantages of the former.

Let G be a set of points defined in $\mathbb{Z}^N$. The *Voronoi neighborhood in G* of any element g of G is defined as

$$N_G(g) = \left\{ v \in \mathbb{R}^N \mid \text{for all } \ h \in G, \|v - g\| \leq \|v - h\| \right\}, \tag{3}$$

i.e., the Voronoi neighborhood of g consists of all points that are not nearer to any other point of G than they are to g. *Voxels* are the Voronoi neighborhoods associated with a grid in three-dimensional space.

Algorithm 1 Multiseeded segmentation algorithm.

```
1   for c ∈ V
2       do for m ← 0 to M
3           do σ_m^c ← 0
4   H ← ∅
5   for m ← 1 to M
6       do for c ∈ V_m
7           do if σ_0^c = 0 then H ← H ∪ {c}
8              σ_0^c ← σ_m^c ← 1
9   l ← 1
10  while l > 0
11      for m ← 1 to M
12          do while V_m ≠ ∅
13              do remove a spel d from V_m
14                 C ← {c ∈ V | σ_m^c < min(l, ψ_m(d, c))}
15                 while C ≠ ∅
16                     do remove a spel c from C
17                        t ← min(l, ψ_m(d, c))
18                        if l = t and σ_m^c < l then V_m ← V_m ∪ {c}
19                        if σ_0^c < t then
20                            if σ_0^c = 0 then H ← H ∪ {c}
21                            for n ← 1 to M
22                                do σ_n^c ← 0
23                        if σ_0^c ≤ t then σ_0^c ← σ_m^c ← t
24      while Maximum-Key(H) = l
25          Remove-Max(H)
26      l ←Maximum-Key(H)
27      for m ← 1 to M
28          V_m ← {c ∈ H | σ_m^c = l}
```

The cubic grid G is $G = \{(c_1, c_2, c_3) \mid c_1, c_2, c_3 \in \mathbb{Z}\}$, (where Z is the set of integers). The voxels of G are cubes of unit volume. The fcc grid F is $F = \{(c_1, c_2, c_3) \mid c_1, c_2, c_3 \in \mathbb{Z} \text{ and } c_1 + c_2 + c_3 \equiv 0 \pmod 2\}$. The voxels of F are rhombic dodecahedra (polyhedra with 12 identical rhombic faces) of twice unit volume. We define the *adjacency* β for the grid F by: for any pair (c, d) of grid points in F, $(c, d) \in \beta \Leftrightarrow \|c - d\| = \sqrt{2}$.

A grid point c has 12 β-adjacent grid points in F. In fact, two grid points in F are adjacent if, and only if, the associated voxels share a face. This fact points to the first advantage of the fcc grid: only a single adjacency relation β need to be used in computing the fuzzy connectedness. If we were using the cubic grid, then, for a grid point c, we may need to use several fuzzy affinity functions: ψ_{mf} for grid points whose voxels share a face, ψ_{me} for grid points whose voxels share an edge and ψ_{mc} for grid points whose voxels share a corner.

The fcc grid with the adjacency β forms a 1-*simply connected* digital space and boundaries in such digital spaces are automatically *Jordan surfaces* [8]; i.e., there is no path from a voxel $a \in A$ to a voxel $b \in B$ (where A and B are two different digitally connected objects) without crossing the boundary between A and B. The reader should consult [11] for a description of an efficient algorithm for boundary tracking in the fcc grid.

Another advantage of the fcc grid is that if we have an object made up from voxels on this grid, for any two boundary faces that share an edge, the normals of these faces make an angle of 60° with each other, resulting in a less blocky image than if we used a surface based on the cubic grid with voxels of the same size. This can be seen in Fig. 1, where we display approximations to a sphere based on different grids. Note that the display based on the fcc grid (b) has a better representation than the one based on cubic grid with the same voxel volume (a) and is comparable with the representation based on cubic grid with voxel volume equal to one eighth of the fcc voxel volume (c). This points to another advantage of fcc grids when compared to cubic grids: fewer grid points are necessary to obtain a comparable digital representation of a volume [11].

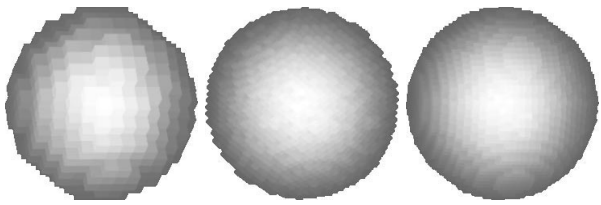

Fig. 1. Computer graphic display of a sphere using different grids. (a) is the display based on a cubic grid with voxels of the same volume as the display based on a fcc used for (b). The image (c) corresponds to a display based on a cubic grid with voxels of volume equal to one eight of the voxel volume in the other two images.

One might argue that the example of Fig. 1 is not general. In fact, we can choose a cube whose size is a multiple of the cubic grid voxel size and get a perfect representation of it as a collection of cubic voxels, but the same cannot be done with the fcc grid. However it is this latter example that is misleading, one can prove the general superiority of the fcc grid over the cubic grid for digital approximations of continuous functions (the fcc grid is said to be more *efficient* than the cubic grid). For a more detailed discussion of fcc and cubic grid efficiencies, the reader should consult [12] and [13].

4 Experimental Results and Discussion

In this section we show experiments that demonstrate the applicability of using the multiseeded fuzzy segmentation algorithm on the face centered cubic grid. For accuracy results and comparisons with other segmentation techniques for two-dimensional images, the reader can refer to [6].

The volumes used in the first segmentation experiments are PET reconstructions (with approximately 5,500,000 voxels) obtained using real data collected from a HEAD PENN-PET scanner, and the RAMLA algorithm for 2.5D [14] was used for reconstruction. The spatial resolution of the scanner used is $3.5 \times 3.5 \times 3.5\,mm$ FWHM. The phantom consists of 6 spheres with walls $1mm$ thick, where 2 are filled with cold (non-radioactive) and 4 are filled with hot (radioactive) water immersed in warm water (the concentration ratio between the hot spheres and the background is 8:1). The two cold spheres have diameters of 28 and $37mm$ and the hot spheres have diameters of 10, 13, 17 and $22mm$. In order to determine the robustness of the segmentation algorithm on this volume two of the authors and another user independently selected seeds for six fuzzy objects: one representing the two cold spheres, one for each one of the four hot spheres and one for the material in which they are immersed. The reason why we selected seeds for the hot spheres as separate fuzzy objects is that, although they have the same physical activity inside them, the reconstructed activity for each one is different due to inaccuracies in the data collection and reconstruction. The results were compared based on the volumes of the detected objects (Table 1).

Table 1. Comparison of actual and detected fuzzy object volumes (in cm^3) corresponding to seed selection by three users. (The first two columns correspond to the two cold objects and the last four columns correspond to the hot objects)

	Cold		Hot			
Actual	24.9	10.8	5.2	2.4	1.1	0.5
User 1	14.3	4.0	13.6	6.8	4.6	1.2
User 2	13.8	4.6	15.0	7.8	5.0	1.1
User 3	12.6	3.3	13.7	6.7	3.8	0.6

In this experiment we are measuring the robustness of the algorithm when receiving inputs from different users. The volume to be segmented is noisy and has low contrast, thus when we compare the volumes of the detected spheres with their actual sizes we are measuring the accuracy of the whole process, from scanning through reconstruction to segmentation. The detected volumes of cold and hot spheres have to be interpreted differently because of

the physical properties [15] of the imaging device used. In PET, a positron generated in a hotter region often migrates to a neighboring colder region before annihilation, but the reverse is less likely to happen. For this reason, we should expect an increase in the apparent volume of the hot spheres and a decrease in the apparent volume of the cold spheres in a reconstruction.

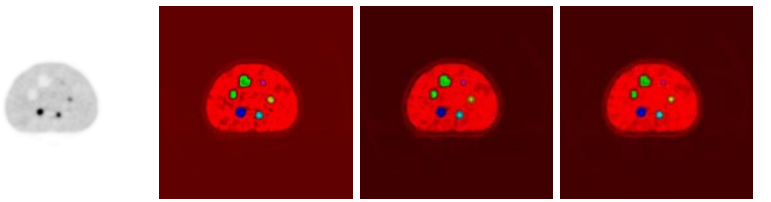

(a) (b) (c) (d)

Fig. 2. Central slice of reconstructed phantom (**a**) and of the segmentations by the three users ((**b**), (**c**) and (**d**))

In Fig. 2 we show the central slice of the reconstructed phantom (a) and of the segmentation by the three users (b, c and d). In the cases of (b), (c) and (d), the hue indicates the object to which the voxel belongs (i.e., the m such that $\sigma_m^c = \sigma_0^c > 0$) and the intensity indicates the grade of membership (i.e., it is proportional to σ_0^c. The phantom slice showed in Fig. 2(a) had its gray levels inverted and adjusted in order to make all objects of interest visible. The average CPU time needed for segmenting the volume consisting of approximately 5,500,000 voxels using a Pentium III (450 MHz) was 7.5 minutes.

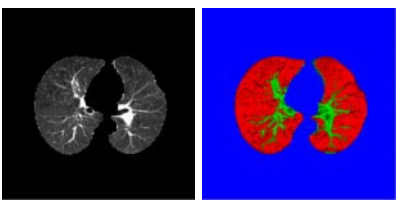

(a) (b)

Fig. 3. Slice of CT volume (**a**) and of the segmentation (**b**)

In the second experiment we make use of the algorithm to segment the blood vessels inside the lungs, dividing the volume in three objects, the spels belonging to lung tissue (colored as red), blood vessels (green) and backgroud (blue). The user identified some points inside the three objects, providing the algorithm with the input needed. Since there is no ground truth, the quality of the segmentation is subjective and has to be assessed by a specialist.

The volume used for this experiment was collected using a CT (Computerized Tomography) scanner, with a spatial resolution of $1.0 \times 1.0 \times 5.0\,mm$ and interpolated to the FCC grid.

In Fig. 4 we show a slice of the reconstructed volume (a) and of the segmentation (b). Again, in the case of (b), the hue indicates the object to which the voxel belongs (i.e., the m such that $\sigma_m^c = \sigma_0^c > 0$) and the intensity indicates the grade of membership (i.e., it is proportional to σ_0^c). The volume slice showed in Fig. 4(a) also had its gray levels inverted and adjusted in order to make all objects of interest visible. The segmentation was evaluated by a pulmonary radiologist who judged it to be accurate except for some overestimation of blood vessels that can be removed by thresholding the conectedness map. The CPU time needed for segmenting the volume consisting of approximately 3,500,000 voxels using a Pentium III (450 MHz) was slightly under 3 minutes.

5 Conclusion

Multiseeded fuzzy segmentation is a semi-automatic method that allows the segmentation of multiple objects in images/volumes containing noise and/or shading. If the user chooses one of the objects to be the background in the volume (as in Fig. 2), then the fuzzy segmentation is achieved without any thresholding.

In this paper we showed that this method can be used to, within a reasonable time, perform segmentation on a poor contrast volume produced by PET reconstructions or on CT data using the fcc grid. The CPU time needed to perform the segmentation is especially important since our technique is semi-automatic, thus the user may wish to add, delete or change seeds after a first segmentation to achieve a better result.

The choice of the fcc grid was based on the facts that fewer grid elements have to be used to represent the same volume with similar accuracy than using a cubic grid and that only one adjacency (the face adjacency) is involved in the computation of the fuzzy affinity function values ,while in a cubic grid we may have as many as three different adjacencies involved at the same time (face, edge and corner adjacencies).

The results of the experiments shows that even when applied to a volume with very poor contrast, the volumes of the segmented fuzzy objects based on inputs from three different users are similar, and, when applied to a lung volume, it was able to segment blood vessels from lung tissue.

The selection of the seeds is a very important step of the process, it is there that the user gives the algorithm her/his high-level knowledge about

the volume to be segmented. Our current work includes experiments whose intent is the determination of the best way to automatically select the seeds for the objects. This has to be application specific, in order to incorporate the high-level knowledge about the properties of the objects.

References

1. Dellepiane S.G., Fontana F., and Vernazza G.L. Nonlinear image labeling for multivalued segmentation. IEEE Trans. Image Process. 1996; 5:429–446
2. Udupa J.K., Wei L., Samarasekera S., Miki Y., van Buchem M.A., and Grossman R.I. Multiple sclerosis lesion quantification using fuzzy-connectedness principles. IEEE Trans. Med. Imag. 1997; 16:598–609
3. Moghaddam H.A. and Lerallut J.F. Volume visualization of the heart using MRI 4D cardiac images. J. Comput. Inform. Tech. 1998; 6:215–228
4. Carvalho B.M., Gau C.J., Herman G.T., and Kong T.Y. Algorithms for fuzzy segmentation. Pattern Anal. Appl. 1999; 2:73–81
5. Rosenfeld A. Fuzzy digital topology. Inform. and Control 1979; 40:76–87
6. Herman G.T. and Carvalho B.M. Multiseeded segmentation using fuzzy connectedness. IEEE Trans. Pattern Anal. Mach. Intell., to appear
7. Udupa J.K. and Samarasekera S. Fuzzy connectedness and object definition: Theory, algorithms and applications in image segmentation. Graph. Models Image Proc. 1996; 58:246–261
8. Herman G.T. Geometry of Digital Spaces. Birkhäuser, Boston, MA, 1998
9. Udupa J.K., Saha P.K., and Lotufo R.A. Fuzzy connected object definition in images with respect to co-objects. In: K.M. Hanson (ed) Image Processing, volume 3661 of Proc. SPIE, 1999, pp 236–245
10. Cormen T.H., Leiserson C.E., and Rivest R.L. Introduction to Algorithms. MIT Press, Cambridge, MA, 1990
11. Garduño E., Herman G.T., and Katz H. Boundary tracking in 3-D binary images to produce rhombic faces for a dodecahedral model. IEEE Trans. Med. Imag. 1998; 17:1097–1100
12. Matej S. and Lewitt R.M. Efficient 3D grids for image reconstruction using spherically-symmetric volume elements. IEEE Trans. Nucl. Sci. 1995; 42:1361–1370
13. Natterer F. The Mathematics of Computerized Tomography. John Wiley & Sons, Chichester, England, 1986
14. Obi T., Matej S., Lewitt R.M., and Herman G.T. 2.5D simultaneous multislice reconstruction by series expansion methods from Fourier-rebinned PET data. IEEE Trans. on Med. Imag. 2000; 19:474–484
15. Bendriem B. and Townsend D.W., editors. The Theory and Practice of 3D PET. Kluwer Academic Publishers, Dordrecht, The Netherlands, 1998